SCIENCE & GLOBAL SECURITY
2023, VOL. 31, NOS. 1–2, 16–40
https://doi.org/10.1080/08929882.2023.2223832

Routledge
Taylor & Francis Group

Simulating the Passive Neutron and Gamma Signatures of Containerized Nuclear Warheads for Disarmament Verification

Svenja Sonder, Carina Prünte, Yannick Fischer, Manuel Kreutle, Jan Scheunemann, and Gerald Kirchner

Carl-Friedrich von Weizsäcker-Center for Science and Peace Research (ZNF), Universität Hamburg, Hamburg, Germany

ABSTRACT

For nuclear disarmament verification, measuring passive neutron and gamma signatures is discussed for confirming the presence of weapons-grade plutonium. Using the Geant4 code, the effects of neutron and photon interactions with the various materials of containerized items are explored for (i) notional fission and thermonuclear warheads waiting for dismantlement, (ii) intentionally shielded plutonium in a scrap container. Due to strong neutronic linking of the various warhead materials neutron multiplicity measurements can not be expected to give correct results. Gamma emissions of the plutonium may even be completely shielded by a tamper. Gamma spectrometry could verify the presence of explosives from (n,γ) activation of hydrogen and nitrogen as well as of fission processes from their prompt fission gamma emissions. Limiting diameters of scrap containers together with long-time gamma measurements of the absence of photons produced by (n,γ) activation of shielding materials will provide an effective approach for detecting an intentional diversion of plutonium.

ARTICLE HISTORY
Received 5 January 2022
Accepted 26 March 2023

Background

Since the end of the Cold War, various studies documented concepts and technologies suitable for nuclear disarmament verification.[1] However, generally accepted concepts for verification of a future treaty on general and complete disarmament under strict and effective international control as called for in Article VI of the Treaty of Nonproliferation of Nuclear Weapons are still missing. If we consider the large numbers of nuclear warheads existing globally and the times needed for dismantling every warhead,[2] efficient, cost-effective procedures should be developed. As a result, measurements may be limited to process steps at which they contribute

CONTACT Gerald Kirchner gerald.kirchner@uni-hamburg.de Carl-Friedrich von Weizsäcker-Center for Science and Peace Research (ZNF), Universität Hamburg, Beim Schlump 83, 20144 Hamburg, Germany.

significantly to the inspectors' confidence applying robust and reliable technologies.

Within this framework, utilizing the passive gamma and neutron emissions of plutonium[3] is highly attractive. Combined with information barriers for preventing a disclosure of sensitive information, this application is generally suggested.[4] The potential of both radiative emissions for attribute and template measurements and for radiation imaging has been studied extensively during the last decades.[5] Whereas the use of templates focuses on gamma-spectrometry,[6] measurement of the plutonium-240:plutonium-239 ratio by gamma spectrometry and of the plutonium-240 mass by neutron multiplicity counting have been repeatedly proposed[7] for verifying weapon specific attributes, usually the presence, mass and isotopic vector of the plutonium.

For assembled warheads it has been pointed out[8] that gamma and neutron signatures are modified by interaction with their components, causing attenuation, thermalization as well as warhead specific (n,γ) signals. However, the potential effect of these processes on the suggested attribute measurements has not yet been systematically explored. For testing them, bare or only slightly shielded plutonium configurations have generally been used.[9] At present, there is a sound basis for verifying the presence of a plutonium pit after dismantlement, but only a limited number of studies analyze the effect of warhead materials on their gamma and neutron signatures.[10]

Evaluation of neutron multiplicity detector count rates is based on various assumptions on the nuclear processes[11] including: (1) emission of the neutrons generated by a spontaneous fission of plutonium-240 and from all fissions induced by this event is instantantaneous (the superfission model), (2) neutron absorption rates other than those inducing fission are negligible, (3) neutron emission is spacially uniform (the point model), and (4) neutron reflection into the fissile material is neglegible. For configurations known to deviate from these assumptions, calibration with reference samples and comparing Monte Carlo simulations of the expected multiplicity count rates with measurements offer suitable procedures for verifying declarations in nuclear safeguards applications.[12] This approach can not be applied to nuclear warhead verification, since the information on nuclear warhead structures and materials required for those simulations are sensitive and will be classified by the nuclear weapon states. Thus, there is a requirement to evaluate whether the impact of warhead materials is limited or may invalidate neutron multiplicity measurements of assembled warheads.[13]

Some notional models of nuclear warheads have been proposed and studied,[14] and the Fetter et al. plutonium model has been used repeatedly

for assessing disarmament verification techniques.[15] However, analyses based on these notional warhead models should not be generalized, as they assume a fission device containing an uranium tamper, which modifies or even effectively shields the passive radiation signals. Therefore, a second notional model is presented which may be more typical of modern thermonuclear weapons. For the Fetter at al. model, a potential hoax is considered; it is assumed that the plutonium is replaced by a californium-252 source with corresponding neutron activity.[16]

In this study, analyses of the interactions of passively generated neutrons and photons within the Fetter et al. model and the two-stage notional warhead are presented and compared. For neutrons, reaction rates within individual components, flux densities inwards and outwards, energy distributions, gamma emissions resulting from neutron interactions within the various warhead components and neutronic coupling between primary and secondary of our two-stage model are evaluated. As nuclear weapons will be present in containers that protect visible sensitive information, its effect on the passive neutron and gamma signals is also quantified. To our knowledge, such data are not available in the open literature[17] but are required for generalizing findings beyond the scope of a notional model. The effect of safety regulations for fully assembled nuclear warheads[18] on such measurements is evaluated. Implications on the use of passive radiation measurement technologies for confirming the *presence* of a plutonium based nuclear warhead are discussed.

During the development of verification concepts within the International Partnership on Nuclear Disarmament Verification and the NuDiVe exercise[19] a second scenario has been identified, where passive gamma and neutron measurements are highly attractive: after warhead dismantlement, verifying the *absence* of plutonium in process rooms and in containers, which are declared to include high explosives or scrap, will be required to confirm that even small, potentially intentionally shielded fractions are not being diverted. A generic model for analyzing this scenario will be presented and gamma and neutron signals will be calculated.

Materials and methods

Scenario (1): Containerized nuclear explosive device

For a notional implosion-type weapon the weapons-grade plutonium model suggested by Fetter et al.[20] was adopted ("Configuration 1") but some of its material compositions were slightly modified. Aged weapons-grade plutonium with ingrowth of the strong gamma emitter americium-241 and TATB (1,3,5-triamono-2,4,6-trinitrobenzene) as typical high explosive[21]

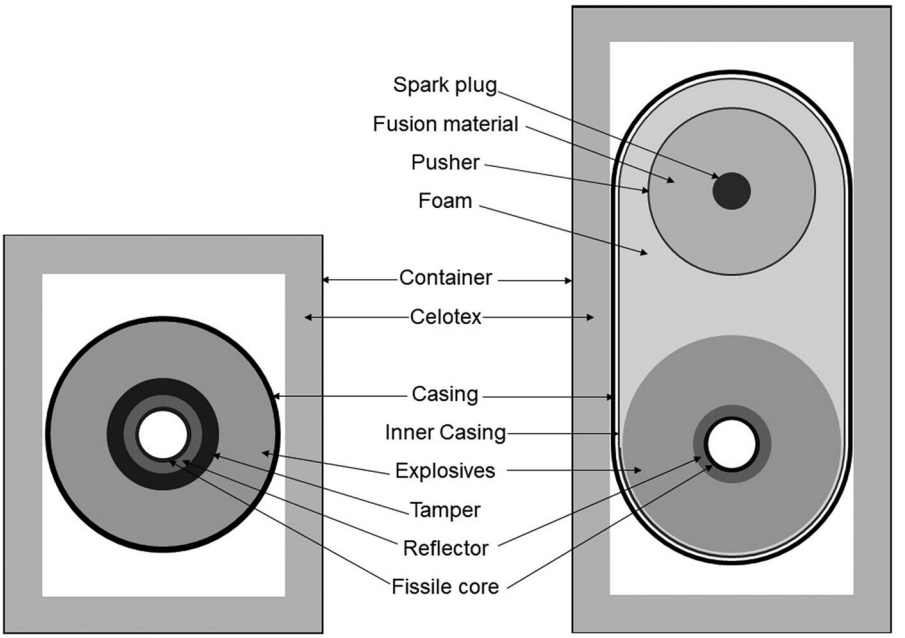

Figure 1. Structure and material compositions of the notional one-stage (left) and two-stage (right) warhead models assumed.

instead of a generic element ratio were assumed. The effect of replacing the plutonium by a californium-252 source was also explored.

Our notional thermonuclear warhead model ("Configuration 2") includes the Fetter et al. model as primary, but without uranium tamper. For its secondary 20 kg HEU (95% enrichment)[22] with ingrowth of decay products for 30 years are assumed. Its other materials and dimensions reflect generic unclassified information,[23] including a thin uranium casing as speculated by Fetter et al.[24]

These notional nuclear warheads were assumed to be present in cylindrical containers with 28.5 cm outer radius and heights of 71 cm and 112 cm, respectively, having an outer steel wall of 0.3 cm thickness surrounding a 6.6 cm cylindrical insert made of Celotex.[25] The nuclear weapon is simulated to be positioned in the center of the container. Details are given in Figure 1 and in Tables A1 and A2.

Scenario (2): Small mass of shielded fissile material

Presumably, verification of a future nuclear disarmament agreement will require preventing an undetected intentional diversion of some fraction of the fissile material. Its mass was arbitrarily set to 50 g of plutonium with the isotopic composition assumed for the implosion-type weapon and with spherical geometry. It is reasonable to suppose that in such a hypothetical

scenario the fissile material will be heavily shielded. In a first series of simulations, the effectiveness of various potential neutron shielding materials (high-density polyethylene (HDPE), cadmium, borated HDPE with boron fractions from 5% to 50%) has been evaluated by increasing their thickness around the plutonium sphere and combining them, until the neutron signal was reduced almost completely. These results were used to simulate the presence of the small plutonium sphere in a standard waste drum filled with scrap metal originating from dismantling (Table A3) and to evaluate whether replacing scrap with the shielding materials could mask either the neutron or the gamma emission or even both.

Neutron and gamma simulations

All simulations were performed using the Monte Carlo Code Geant4,[26] versions 10.5 and 10.6. Originally developed at CERN for high energy physics detector design, this code has become a frequently used tool in nuclear safeguards and disarmament verification research.[27] In general, a neutron cross section library based on ENDF/B-VIII.0 was used, only the scattering cross sections of thermalized neutrons at bound hydrogen available with Geant4 in file G4NeutronHPThermalScatteringData are based on ENDF/B-VII.1. All simulations used the LLNL fission model.[28]

Photon data were taken from the G4EmStandardPhysics Physics List of Geant4, which also provides the data required for simulating their interaction with matter. For each of the fissionable materials simulations were confined to the 100 gamma lines showing the highest branching ratios. This covers 99.99% of the total disintegrations of plutonium and 98.5% of uranium. Photons emitted by bismuth-214 and lead-214 are not considered, since emanation of their noble gas precursor radon-222 from soil, rock and building materials will create elevated background concentrations of these short-lived isotopes in air. Data for prompt fission gammas are provided by the LLNL fission model.

Although considerable work has been done to validate Geant4,[29] the code still has some shortcomings in its treatment of neutron cross sections, which could bias the simulations performed in this study.[30] Therefore, additional simulations were run for configurations, which are comparable to those considered in this study and for which either experimental data or results from reference codes' simulations are available. These included the ICSBEP[31] benchmark criticality experiments PU-MET-FAST-002 ("Jezebel") and HEU-MET-FAST-001 ("Godiva"), which represent fast neutron spectra originating from metallic plutonium and highly enriched uranium (HEU), respectively. For both, the simulated[32] effective neutron multiplication factor k_{eff} showed only small negative deviations from

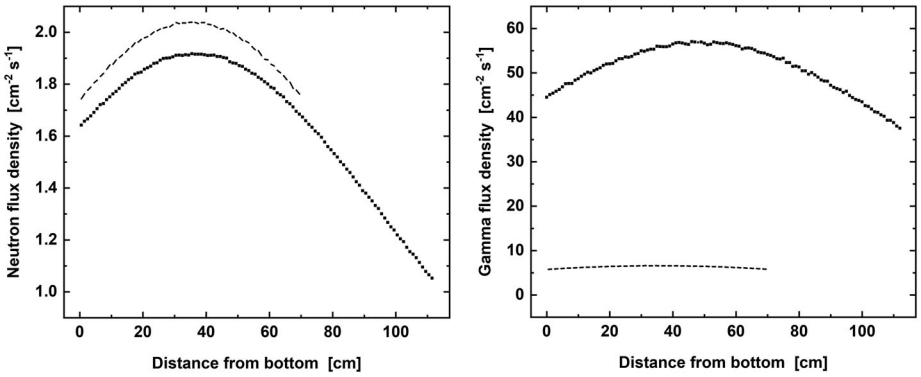

Figure 2. Simulated axial neutron (left) and gamma (right) flux densities at 1 m distance from the surface of the container with a notional warhead inside. Dashes: Configuration 1, squares: Configuration 2.

criticality ($\leq$0.6%). Code-to-code comparisons of Geant4 with MCNP[33] and SCALE/KENO-VI[34] were performed for simulations of a large number of plutonium-uranium mixed oxide configurations with varying shieldings and reflectors (bare, cadmium, lead, HDPE), which cover a wide range of masses, plutonium concentrations, and isotopic compositions. Reactivities calculated by Geant4 are within the variability of the two Monte Carlo reference codes but calculate higher neutron flux densities of the HDPE configurations at energies below 0.1 eV.[35]

Results and discussion

Scenario (1): Containerized nuclear explosive device

Neutron emissions. For the primaries of the notional warhead models, a neutron source term of 2.8 $\cdot 10^5$ s^{-1} is calculated, of which 68% originate from spontaneous fission of the plutonium-240. Simulated neutron flux densities along the axis of loaded containers at 1 m distance are shown in Figure 2 (left). Even if the background is significantly elevated compared to its cosmogenic level,[36] this signal will easily be detected by commercially available helium-3 neutron detectors. For the two-stage model, the position of the maximum reflects that 94% of the fission events are within the plutonium of the primary, 4% within the HEU and the remaining 2% within the uranium casing.

Neutron interaction processes

Geant4 allows extracting information on the neutron physics within the configurations, which is compiled in Table 1 for Configuration 1. The noticeable effect of TATB on neutron scattering reflects both the high cross

Table 1. Neutron interactions within a hypothetical warhead (Configuration 1) and its container; missing entries denote fractions <0.1%.

	Fraction of neutron processes[a] [%]			
Material	Elastic scattering	Inelastic scattering	Absorption	Induced fission
Pu	2.2	14.5	9.4	71.7
Be	9.8	1.0		
U	12.7	59.7	58.3	28.3
TATB	70.4	24.2	22.4	
Al	0.4	0.3	1.4	
Celotex	4.0		2.2	
steel	0.5	0.3	6.3	

[a]100% correspond to total interactions per reaction type.

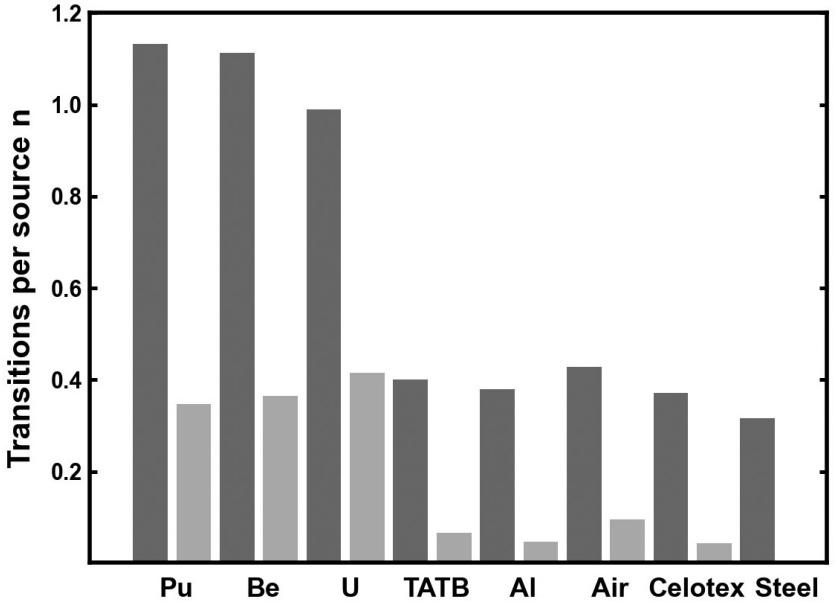

Figure 3. Mean number of passes in the notional fission warhead (Configuration 1) per neutron emitted by the plutonium across the various material interfaces to the outside (dark gray) and inward (light gray).

section of the hydrogeneous material and its high mass. These findings confirm and quantify the considerations[37] of potential effects of the weapons' components. Their presence results in a strong neutronic linking of the fissile material not only with reflector and tamper (if present), but also with the high explosives. For Configuration 1, merely 2% of the neutrons escape without any interaction. As Table 1 indicates, more than 30% of the neutron absorptions occur in non-fissile material. This strongly violates the assumption that this fraction is negligible made in the point model[38] used for evaluating neutron multiplicity measurements.

As shown in Figure 3, major fractions of neutrons are reflected back by the warhead materials with approximately every second neutron passing the uranium/TATB interface being backscattered by the high explosives.

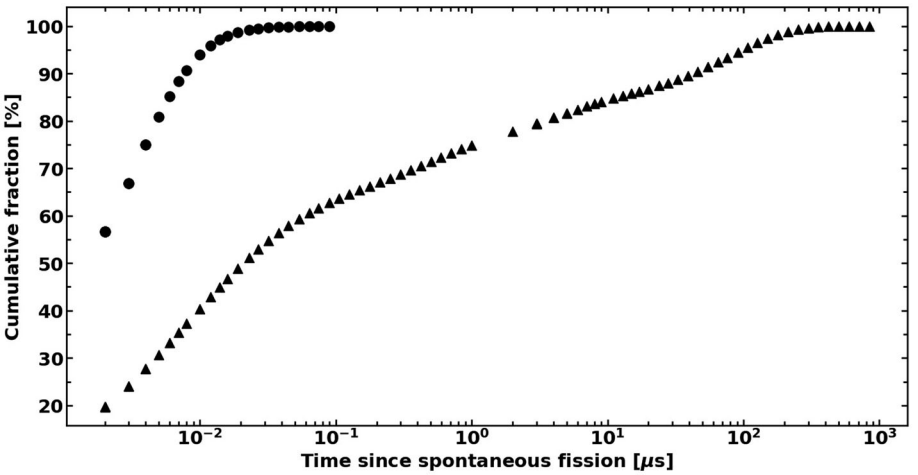

Figure 4. Cumulative distribution of times passed between spontaneous fission of a plutonium-240 nucleus and fissions induced by this event in plutonium of the notional thermonuclear warhead (triangles) and its bare plutonium hollow-sphere (circles).

This effect also has major implications on neutron multiplicity measurements. First, it results in increased flux densities and fission rates in the outer region of the plutonium,[39] which is not in accordance with the point model assumption that these are spatially uniform. Second, 25% of the fissions in plutonium-239 are induced by backscattered neutrons. The consequences are illustrated in Figure 4, which shows the dynamics of the fission chains triggered by the spontaneous fission of a plutonium-240 isotope. Whereas fissions are almost instantaneous for the bare plutonium hollow sphere, more than 25% of the induced fissions are delayed by 1 μs in the notional warhead, 15.6% by even more than 10 μs. The superfission model commonly used for evaluating neutron multiplicity count rates is adequate for bare plutonium, but becomes questionable for configurations showing enhanced neutron moderation and backscattering.

The various neutron sources and their contributions to the flux densities of Figure 2 (left) are listed in Table 2. As expected, spontaneous and induced fission neutrons of plutonium dominate, but for Configuration 1 induced fission in the uranium tamper contributes about 15% to the neutron signal. The considerable number of targets and reaction types displayed in Table 2 again reflect the strong neutronic linking between the materials of the primary of both notional warhead models. These results provide detailed insight into the impact on neutron interactions with warhead materials addressed earlier.[40] A general shift is apparent from neutrons generated in components inside of the high explosives toward neutrons emitted by other materials. It reflects the high absorption rates by the hydrogeneous material (Table 1). Although these data are based on notional warhead models, they indicate two general implications for

Table 2. Production modes and materials of the neutrons emitted from the container loaded with a notional warhead of Configuration 1 and Configuration 2, respectively.

Material			Fraction of neutrons[a] [%]			
			Configuration 1		Configuration 2	
Source	Target	Reaction	Generated	Emitted	Generated	Emitted
Pu	–	SF	26.8	25.9	30.2	29.3
Pu	Pu	(n,f)	47.1	45.4	59.1	57.7
Pu	U_{nat}	(n,f)	12.5	15.2	0.9	2.5
Pu	U_{nat}	(n,2n)	0.2	0.2		
Pu	Be	(n,2n)	4.4	3.5	5.3	3.6
Pu	HEU	(n,f)	–	–	1.7	3.6
U_{nat}	Pu	(n,f)	2.6	2.5		
U_{nat}	U_{nat}	(n,f)	3.8	4.6		
U_{nat}	Be	(n,2n)	0.3	0.3		
HEU	HEU	(n,f)	–	–	0.3	0.6
Be	Pu	(n,f)	1.6	1.6	2.3	2.2
Be	U_{nat}	(n,f)	0.6	0.8		0.2
Be	HEU	(n,f)	–	–	0.1	0.2

[a]Fractions <0.1% are not specified.

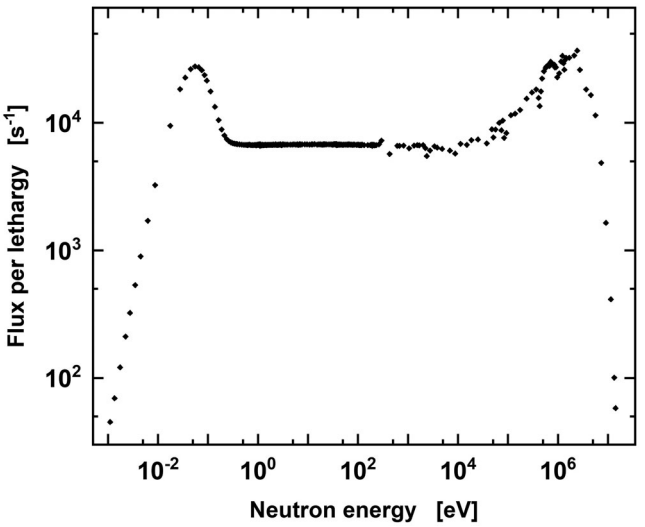

Figure 5. Energy distribution of neutrons emitted by the containerized notional warhead of Configuration 1.

neutron multiplicity measurements of warheads. Since additionally to spontaneous fission of plutonium-240 induced fission in plutonium-239 and in case of a tamper also in uranium provides major fractions of the neutron source term, a weighted average of the multiplicity distributions caused by these processes should be used. If a beryllium reflector is present, (n,2n) processes in this material will produce a significant fraction of correlated neutrons, which needs to be taken into account for avoiding a systematic bias in estimating plutonium masses.

The mean energy distribution of neutrons passing the surface of a container loaded with a Configuration 1 warhead is shown in Figure 5. The

moderating effects of the TATB and, to a lesser extent, of the Celotex layer become immediately apparent. In the case of a Configuration 2 warhead, the energy distribution is similar with 25–30% lower neutron fluxes at energies below 10 keV. The strong moderating effect of the TATB indicates the option to verify the presence of high explosives by analyzing the energy distribution of the neutrons emitted from an item declared as nuclear warhead, e.g. by a Bonner sphere detector. Since scattering of unmoderated fission spectrum neutrons by building walls results in a spectrum similar as in Figure 5,[41] effective shielding of such back-scattered neutrons will be mandatory[42] for such measurements. Emission of a thermalized spectrum will reduce the efficiency of neutron detectors compared to fission spectra due to enhanced neutron absorption in the moderator of helium-3 counters. This effect needs to be considered for multiplicity detectors, which usually are calibrated with an unmoderated californium-252 source.

Plutonium replaced by californium-252

The neutron signatures resulting from such a manipulation, which is comparatively easy to realize, have been analyzed for the Configuration 1 warhead model. Since induced fission in small mass sources is not relevant, a spontaneous fission activity of californium-252 twice as high as of the plutonium-240 is required ($4.1 \cdot 10^5$ neutrons per second, corresponding to 0.17 µg) for the same neutron source term. Such a hoax will produce almost identical neutron flux densities and energy distributions at the container surface (data not shown). Thus, combining neutron flux analyses with a second technology[43] is desirable for verifying the presence of plutonium.

Neutron die-away times. As Figure 4 indicated, neutron interaction processes with warhead components have the potential to modify the emission dynamics of fission neutrons. Times required for selected cumulative fractions of the neutrons of the fission chains, which are produced by spontaneous fission of plutonium-240, until they pass the outer surface of the various components of the notional thermonuclear warhead are compiled in Table 3, their distribution is shown in Figure 6 for the neutrons leaving the container. Neutron residence times are significantly modified by the high explosives and to a lesser extent by the celotex, but not by any of the other components. As Figure 6 illustrates, emission of the neutrons generated within an identical bare plutonium hollow sphere is completed after 0.1 µs, but this process requires more than 300 µs for the containerized notional warhead.

Two consequences for neutron multiplicity analyses of assembled warheads become apparent from comparing their die-away time (Figure 6) with the common 64 µs multiplicity gate length[44] which takes into account

Table 3. Cumulative fractions of times required by neutrons produced by an Initial plutonium-240 spontaneous fission to pass the Configuration 2 warhead components.

Component	Times required [μs] for fraction of		
	50%	90%	95%
Plutonium	0.02	0.05	0.07
Reflector	0.03	0.09	0.13
High explosives	0.57	142.	210.
Polystyrene foam	0.62	143.	208.
Uranium casing	0.62	143.	207.
Aluminum casing	0.68	145.	210.
Celotex	1.17	191.	283.
Container steel	1.10	195.	295.

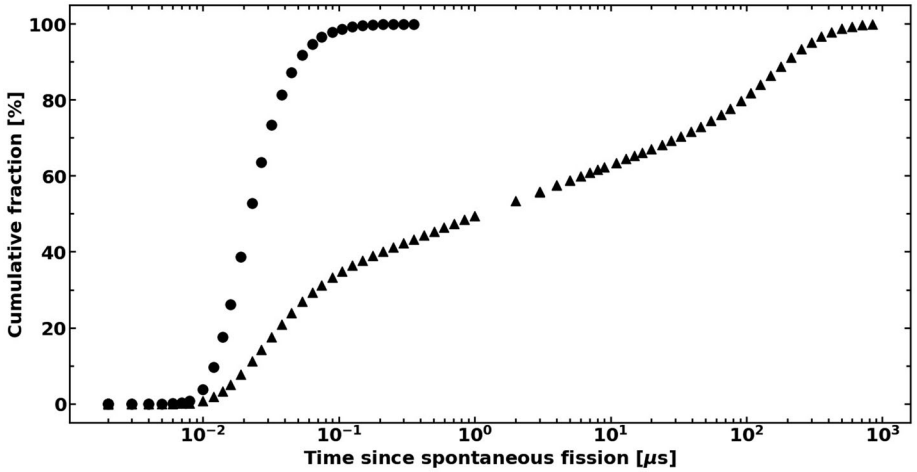

Figure 6. Cumulative distribution of times passed between a plutonium-240 spontaneous fission event and emission of the neutrons of its fission chain from the container for Configuration 2 (triangles) and from its bare plutonium hollow sphere (circles).

the neutron die-away time within the detector. First, other than for bare plutonium only part of the fission chain neutrons generated by a plutonium-240 spontaneous fission will be detected causing a systematic underestimation of its mass.

Correction factors can be established for the celotex or other moderators potentially present in containers from multiplicity measurements of a reference californium-252 source placed inside of the empty container, but not for the high explosives of assembled warheads. Second, neutrons signals produced by subsequent plutonium-240 spontaneous fission processes within the assembled warhead partially overlap[45] resulting in a systematic overestimation of its mass. Even if these two effects with their opposite bias may partially cancel out in neutron multiplicity measurements of warheads, the remaining error can not be quantified without information on materials and dimensions of the analyzed item. However, these parameters

are considered sensitive information[46] and may not be available to inspectors.

Gamma signatures

Axial photon flux densities at 1 m distance from the containers are shown in Figure 2 (right). These signals can be easily detected by hand-held gamma detectors. Table 4 specifies the photon source strengths and emission rates from the container, which are generated by radioactive decay processes within the fissionable materials and by prompt gammas produced by spontaneous and induced fission. Unscattered as well as scattered and secondary photons are included. If a heavy metal tamper is present (Configuration 1), any plutonium gamma signal is suppressed by a factor of $>10^6$. This prevents measurement of the plutonium-240:plutonium-239 isotope ratio by passive gamma spectrometry. A significantly higher photon emission rate originating from plutonium disintegration processes was calculated by Lepowsky et al.[47] It results from the small thickness of the plutonium shell they assumed, which drastically reduces self-absorption rates, and from neglecting other warhead components.

The potential presence of a tamper in warheads has consequences for the use of passive gamma measurements for verification. Attribute measurements based on passive gamma-spectrometry alone may not be sufficient to confirm the presence of plutonium in such weapons. Gamma template measurements could still be performed but would not capture the presence of plutonium. The use of gamma templates for identifying various types of warheads[48] could be limited, if some of these have tampers[49] The presence or absence of a tamper in combination with plutonium should be ruled out by other means.

For Configuration 2, the simulated photon energy distribution and intensities at the axial center in 1 m distance from the container surface are shown in Figure 7. Various marked gamma lines are visible, both at the energy range of the uranium and plutonium decay emissions ($E_\gamma \leq$

Table 4. Photon sources, production and emission rates of the two notional containerized warheads.

	Configuration 1		Configuration 2	
Process	Production Rate [s^{-1}]	Emission Rate [s^{-1}]	Production Rate [s^{-1}]	Emission Rate [s^{-1}]
Pu, decay	$4.0 \cdot 10^{11}$	0	$4.0 \cdot 10^{11}$	$5.3 \cdot 10^{6}$
Pu, fission[a]	$1.4 \cdot 10^{6}$	$7.7 \cdot 10^{3}$	$1.5 \cdot 10^{6}$	$9.9 \cdot 10^{4}$
U_{nat}, decay	$1.0 \cdot 10^{8}$	$1.1 \cdot 10^{6}$	$3.9 \cdot 10^{7}$	$2.9 \cdot 10^{6}$
U_{nat}, fission[a]	$3.3 \cdot 10^{5}$	$1.4 \cdot 10^{4}$	$1.8 \cdot 10^{4}$	$6.8 \cdot 10^{3}$
HEU, decay	–[b]	–	$1.6 \cdot 10^{9}$	$1.7 \cdot 10^{6}$
HEU, fission[a]	–	–	$3.8 \cdot 10^{4}$	$9.0 \cdot 10^{3}$

[a]Prompt fission gammas. [b]–: material not present in Configuration 1.

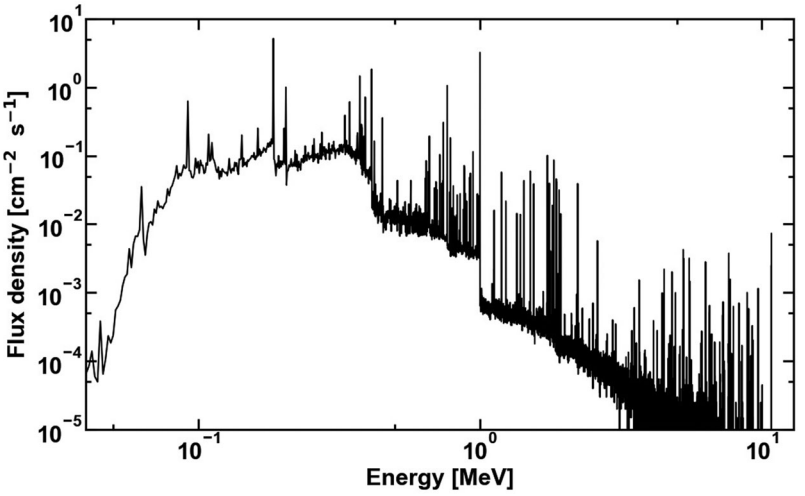

Figure 7. Energy distribution and intensities of gammas at 1 m distance from the Configuration 2 warhead container.

1 MeV) and at energies above 2 MeV caused by prompt (n,γ) activation processes in weapon and container materials. In addition the marked continuum of photons at high energies up to 10 MeV caused by prompt fission gammas confirms the presence of spontaneous fissioning materials, but not necessarily of plutonium-240.

Flux densities at a distance of 1 m from the surface of the container are listed in Table 5 for the most prominent lines, which are of interest for nuclear warhead verification. As their intensities in particular at low energies may crucially depend on the thickness of the uranium casing, Table 5 also includes gamma flux densities for a 5 mm uranium casing. These were calculated from the 1 mm casing results using the mass attenuation coefficients given by Reilly.[50] They indicate that the presence of plutonium as well as of explosives can be verified gamma-spectrometrically for the notional thermonuclear warhead even for a 5 mm casing as well as estimating its plutonium-240:plutonium-239 isotope ratio, although this may require extended measurement times.[51] Verifying the presence of uranium-235 is hampered by natural radium-226, which in terrestrial environments is found ubiquitously in soils and building materials and which shows a high emission probability decay at 186 keV overlapping with the uranium-235 gamma signal. Since the radium-226 background depends on local geology and may vary significantly,[52] using the uranium-235 decay energy of 205 keV may be attractive. As Table 5 indicates, caution should be exercised in interpreting any uranium-235 signal, since it does not necessarily indicate the presence of HEU, but could partially or even completely result from a natural (or even depleted) uranium casing. The simulated data

Table 5. Photon flux densities of relevant isotopes and their major gamma lines averaged over ±2.5 cm of the vertical center of the notional thermonuclear warhead container at 1 m distance from its surface.

γ Energy [MeV]	Isotope	Flux density [cm^{-2} s^{-1}] 1 mm U	5 mm U
	(a) Decay processes		
0.186	Uranium-235, HEU	4.00	$<10^{-4}$
	Uranium-235, casing	1.13	1.21
0.205	Uranium-235, HEU	0.83	$<10^{-4}$
	Uranium-235, casing	0.13	0.15
0.375	Plutonium-239	1.45	0.14
0.413	Plutonium-239	1.83	0.47
0.451	Plutonium-239	0.35	0.067
0.640	Plutonium-239	0.037	0.014
0.642	Plutonium-240	0.012	$4.6 \cdot 10^{-3}$
0.646	Plutonium-239	0.071	0.027
0.662	Americium-241	0.21	0.083
0.721	Americium-241	0.13	0.056
0.742	Protactinium-234	0.30	0.13
0.766	Protactinium-234m	1.05	0.49
1.001	Protactinium-234m	3.19	1.81
	(b) Activation processes		
2.223	Hydrogen-1 (n,γ)	0.023	0.016
5.269	Nitrogen-14 (n,γ)	$2.5 \cdot 10^{-3}$	$1.8 \cdot 10^{-3}$
10.83	Nitrogen-14 (n,γ)	$5.7 \cdot 10^{-3}$	$3.8 \cdot 10^{-3}$

given in Table 5 are in good agreement with the gamma measurements performed in 1989 during the Black Sea experiment.[53] Since there is no relevant radium-226 background on the open sea, uranium-235 was identified by its 185.7 keV gamma peak.

Figure 7 and Table 5 document that evaluating the high-energy gamma lines caused by activation of hydrogen and nitrogen could be a promising option for verifying the presence of high explosives, in particular, if a gamma analysis is performed for confirming the presence of (military) plutonium. This confirms and quantifies considerations[54] on the potential of neutron activation processes in high explosives for verification. Our results are complemented by Weng and coauthors,[55] who for the Fetter et al. warhead model have shown recently that the prompt gamma emissions caused by (n,γ) reactions in explosives can be detected gamma-spectrometrically even in the presence of a heavy metal tamper.

As these results indicate, gamma templates recorded for nuclear disarmament verification would gain in specificity if count rates of the high explosives (n,γ) reactions and at an energy interval characteristic of prompt fission gammas are recorded together with photons emitted by decay processes of fissile material. Additionally such gamma templates could be used also to verify various attributes (presence of plutonium, its plutonium-239:plutonium-240 isotope ratio, the presence of high explosives)–an option which to our knowledge has not been considered yet.

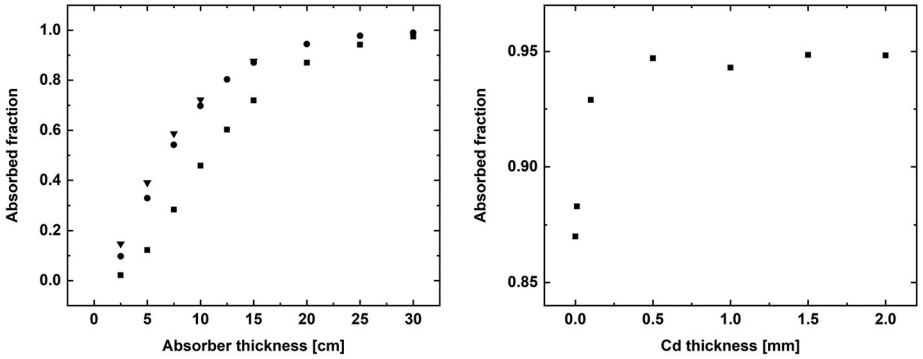

Figure 8. Neutron absorption by various HDPE configurations (left) and by 20 cm HDPE covered by cadmium (right); squares denote pure HPDE, circles homogeneously borated HDPE (5% boron) and triangles a heterogeneous HDPE configuration with 50% boron.

Scenario (2): Small mass of shielded fissile material

Intentional shielding of neutrons

The effect of encasing the plutonium in polyethylene is shown in Figure 8. If its thickness is increased to 30 cm, the neutron flux outside of the configuration is reduced to about 5%. This reflects the moderating effect of the polyethylene combined with the comparatively high absorption cross section of hydrogen for thermalized neutrons. Its efficiency can be even increased by mixing the polyethylene with boron as strong thermal absorber, which at a homogeneous mass fraction of 5% reduces the thickness required for absorbing 95% of the emitted neutrons to 20 cm and for 99% to 30 cm (Figure 8, left). A slightly smaller effect results from covering the polyethylene by a 0.5 mm thick sheet of cadmium (Figure 8, right). Increasing its thickness (Figure 8, right) or the boron concentration of polyethylene (data not shown) becomes ineffective, as the configuration is already deprived of thermalized neutrons. These results suggest to compare the effectiveness of these two configurations with that of a heterogeneous arrangement of borated polyethylene. It was modeled as a layer of pure polyethylene covered by the borated HDPE. Diameters of each layer were adjusted until the summed mass fractions agreed with boron fractions of the corresponding homogeneously borated (5% boron) polyethylene. As expected, heterogeneous configurations are slightly more effective absorbers (Figure 8, left), but differences become negligible for large moderator thickness. This reflects that an increasing ratio of the thermalized neutrons is absorbed by hydrogen before reaching the outer borated polyethylene layer.

Intentional shielding of gamma and neutron signals

As the 50 g of plutonium is assumed to be centered in the waste drum, gamma flux densities at its surface averaged over the ± 2.5 cm around its

axial center are calculated. The results given in Table 6 indicate that already 2.5 cm of lead enclosing the plutonium prevents detecting its gamma signal, unless excessive measurement times combined with effective background suppression are applied. The small volume of lead required for achieving this effect corresponds to a mass of <1% of the scrap present in the drum.

The effect on the neutron signal of covering the 50 g plutonium enclosed in 2.5 cm lead with borated HDPE (5% boron) replacing dismantlement scrap is documented in Table 7. Already with less than 20 cm of this material the fissile material could hardly be detected by scanning the drum with a hand-held detector, since it is close to the cosmic neutron background.[56] However, if the drum will be surrounded by large area neutron detector collars as used for neutron coincidence measurements, the presence of a neutron emitter within the waste will become apparent even with 25 cm of borated HDPE shielding.[57] However, such a configuration will produce additional gamma lines by (n,γ) reactions within the shielding materials. As documented in Table 8, their flux densities are similar to or higher than those of the plutonium decay lines (Table 6, 2.5 cm lead), but show lower background at the high energies of hydrogen and lead. Providing the lead outside of the HDPE shielding would diminish these signals, but almost double the weight of the filled container.

Table 6. Photon flux densities of the major gamma lines of 50 g of plutonium in a filled dismantlement scrap drum averaged over ±2.5 cm around the vertical center of its surface with increasing thickness of lead shielding.

γ Energy [MeV]	Isotope	Source term [s^{-1}]	Self-absorption [%]	No lead flux density [cm^{-2} s^{-1}]	1 cm lead	2.5 cm lead
0.059	Americium-241	$4.6 \cdot 10^{9}$	99.4	0	0	0
0.125	Americium-241[a]	$6.0 \cdot 10^{5}$	98.9	0.046	0.003	<0.001
0.129	Plutonium-239	$6.8 \cdot 10^{6}$	98.8	0.065	0.003	<0.001
0.375	Plutonium-239	$1.7 \cdot 10^{6}$	86.6	1.4	0.067	0.001
0.377	Americium-241	$1.8 \cdot 10^{4}$	83.8	0.065	0.006	<0.001
0.413	Plutonium-239	$1.6 \cdot 10^{6}$	83.9	1.8	0.13	0.005
0.642	Plutonium-240	$2.5 \cdot 10^{3}$	68.8	0.0087	0.004	<0.001
0.646	Plutonium-239	$1.6 \cdot 10^{4}$	69.6	0.060	0.017	0.003
0.662	Americium-241	$4.6 \cdot 10^{4}$	68.8	0.17	0.048	0.007
total		$5.0 \cdot 10^{9}$	99.4	30.	2.4	0.18

[a]With contribution from plutonium-239.

Table 7. Neutron fluxes at the surface of a filled dismantlement scrap drum and flux densities at its vertical center with 50 g of plutonium shielded by 2.5 cm lead and varying thickness of borated HDPE.

HDPE [cm]	Flux [s^{-1}]	Flux density[a] [cm^{-2} s^{-1}]
15	236.6	0.024
20	94.9	0.0097
25	40.4	0.0041

[a]Averaged over ± 2.5 cm surface area around its axial center.

Table 8. Photon flux densities due to (n,γ) processes caused by 50 g of shielded (2.5 cm lead, 20 cm HDPE with 5% boron) plutonium in a filled dismantlement scrap drum averaged over ± 2.5 cm around the vertical center of its surface.

γ Energy [MeV]	Element	Production mode	Flux density [cm^{-2} s^{-1}]
0.478	Boron	^{10}B (n,γ) ^{11}B	0.11
2.223	Hydrogen	^{1}H (n,γ) ^{2}H	0.00083
2.615	Lead	^{207}Pb (n,γ) ^{208}Pb	0.00035

Our results indicate a strategy for verifying that there is no diversion of plutonium via the pathway considered. First, sizes of the waste drums should be confined to about 60 cm in diameter, which prevents excessive shielding by lead, HDPE plus massive layers of scrap. Second, it could be verified that the weight of the filled drum does not exceed reasonable limits. Third, high efficiency gamma and neutron measurements should be performed: increasing an intentional shielding will diminish the primary gamma and neutron signals of diverted plutonium, but increase the number of neutron activation processes and vice versa. These absence measurements will not require information barriers, but high efficiency detectors and long measurement times. However, if the absence of HEU needs to be verified, neutron interrogation analyses will be mandatory which can be applied also for verifying the absence of plutonium in the waste drums.

Conclusions

Our simulations have confirmed that the Geant4 code is a convenient diagnostic tool for analyzing neutron and gamma interactions and flux densities within a containerized nuclear warhead. It allows to extract information hardly gained by measurements. Although this study used notional warhead designs of a plutonium fission and a HEU based thermonuclear warhead, various general conclusions can be drawn.

Neutrons generated within the fissile material of an assembled plutonium warhead show a high probability of interacting with reflector, tamper (if present) and high explosives resulting in an approximately 40% chance of being reflected back. This together with the moderating effect of the high explosives, with (n,2n) reactions in the beryllium reflector, neutron absorption and with high induced fission rates in the plutonium and uranium significantly modifies flux densities, multiplicities and die-away times of the neutrons until they leave the container. As a consequence, neutron multiplicity counting should not be applied for nuclear warhead verification, as the assumptions of the Böhnel point-model generally used for its evaluation are significantly violated. The alternative of comparing experimental data with expected count rates resulting from Monte Carlo simulations is not applicable, as the required detailed warhead design information are classified.

The plutonium decay gammas are completely absorbed within a tampered configuration. This excludes the option of verifying the presence of weapons-grade plutonium by analyzing its isotope ratio gamma-spectrometrically. If there is no tamper, various gamma lines originating from plutonium and uranium decay processes are present outside of the container. This enables verifying the presence of uranium, plutonium and of its plutonium-240:plutonium-239 ratio, but will require long-time measurements due to their low gamma intensities.

Gamma-spectrometric measurements allow to confirm the presence of fission processes from the prompt fission gammas emitted with energies above 2 MeV and of explosives from the high energy photons produced by (n,γ) reactions in hydrogen and nitrogen. These signals should be included in item-specific gamma templates to be used in nuclear disarmament verification.

In case of the hypothetical diversion scenario, which assumes 50 g plutonium being centered in a waste drum filled with dismantlement scrap material, enclosing the fissile material in 2.5 cm lead surrounded by more than 25 cm borated polyethylen effectively masks the gamma and neutron radiation, but produce specific, albeit low intensity gamma signals due to (n,γ) activation of boron, lead and hydogen. Such a diversion can be prevented by limiting the waste drums' diameter to 60 cm combined with long-time (some hours) gamma spectrometric measurements.

Acknowledgements

This work was initiated by and benefited much from the many inspiring and fruitful discussions the corresponding author had during the last years within the *International Partnership for Nuclear Disarmament Verification*. Thanks to all of them, but in particular to Nico van Xanten (Authority for Nuclear Safety and Radiation Protection, The Netherlands) for his continuous interest in the reliability of fissile material absence measurements.

Notes and References

1. These include S. Drell, P. Banks, C. Callan, K. Case, J. Cornwall, F. Dyson, D. Eardley, N. Fortson, M. Freedman, R. Garwin, et al., "Verification Technology: Unclassified Version," JASON, The MITRE Corporation, McLean, VA, USA, 1990; U.S. Department of Energy, Office of Arms Control and Nonproliferation, "Transparency and Verification Options: An Initial Analysis of Approaches for Monitoring Warhead Dismantlement," Washington, DC, USA, 1997; Christine Comley, Mike Comley, Peter Eggins, Garry George, Steve Holloway, Martin Ley, Paul Thompson, Keith Warburton, "Confidence, Security and Verification: The Challenges of Global Nuclear Weapons Arms Control," Atomic Weapons Establishment, AWE/TR/2000/01, Aldermaston, UK, 2000; National Academy of Sciences, "Monitoring Nuclear Weapons and Nuclear-Explosive Materials: An Assessment of

Methods and Capabilities," The National Academies Press, Washington, DC, USA, 2005; David Cliff, Hassan Elbathimy, and Andreas Persbo, "Verifying Warhead Dismantlement - Past, Present, Future," Verification Research, Training and Information Centre (VERTIC), London, UK, https://www.vertic.org/media/assets/Publications/VM9.pdf; Nuclear Threat Initiative, "Innovating Verification: New Tools & New Actors to Reduce Nuclear Risks: Verifying Baseline Declarations of Nuclear Warheads and Materials," Washington, DC, USA, 2014, https://www.nti.org/analysis/articles/innovating-verification-new-tools-new-actors-reduce-nuclear-risks/. Building on this work, the International Partnership on Nuclear Disarmament Verification combines expertise and perspectives of more than 25 countries for developing concepts and procedures, identifying potentially attractive technologies and supporting practical exercises, Corey Hinderstein, "International Partnership for Nuclear Disarmament Verification: Laying a foundation for future arms reductions," *Bulletin of the Atomic Scientist* 74 (2018): 305–11.

2. According to the U.S. Department of Energy it requires 5–21 days depending on the warhead type, https://www.youtube.com/watch?v=SOajFJIzQew.
3. This contribution focuses on plutonium as fissile material, since the neutron source term of HEU is marginal (approx. $1\,s^{-1}\,kg^{-1}$).
4. "Transparency and Verification Options," 76; "Confidence, Security and Verification," 5, 25, 31; "Monitoring Nuclear Weapons and Nuclear-Explosive Materials," 97–108; "Innovating Verification," 31–2, 33–4.
5. These were reviewed by R. C. Runkle, A. Bernstein, and P. E. Vanier, "Securing special nuclear material: Recent advances in neutron detection and their role in nonproliferation," *Journal of Applied Physics* 108 (2010): 111101; Malte Göttsche and Gerald Kirchner, "Measurement Techniques for Warhead Authentication with Attributes: Advantages and Limitations," *Science & Global Security* 22 (2014): 83–110; Jie Yan and Alexander Glaser, "Nuclear Warhead Verification: A Review of Attribute and Template Systems," *Science & Global Security* 23 (2015): 157–70; K. P. Ziock, "Principles and Applications of Gamma-Ray Imaging for Arms Control," *Nuclear Instruments and Methods in Physics Research A* 878 (2018): 191–9.
6. A prominent example is the Trusted Radiation Identification System, Michael Hamel, "The Trusted Radiation Information System (TRIS): Designed to Encourage Trust," INMM Just Trust Me Workshop, Albuquerque, NM, USA, 12–13 March 2019; TRIS discriminated between various warhead and component types in the 1997 radiation signature measurement campaign at the U.S. Pantex plant, see "Monitoring Nuclear Weapons and Nuclear-Explosive Materials," 101.
7. Thomas E. Shea, "Report on the Trilateral Initiative," *IAEA Bulletin* 43 (2001): 49–53; "Confidence, Security and Verification," 18–19, 46–8; "Innovating Verification," 31–32; "Measurement Techniques for Warhead Authentication with Attributes," 87.
8. "Verification Technology," 94, 96; "Transparency and Verification Options," 140; "Confidence, Security and Verification," 18; "Innovating Verification," 32–3, 42.
9. This holds for the results addressed in the reviews cited in note 1 above and for the attribute measurement systems developed cooperatively by Russian and U.S. laboratories, https://www.lanl.gov/orgs/n/n1/FMTTD/presentations/pdf_docs/exec_sum.pdf; Sergey Kondratov, M. Bulatov, D. Decman, M. Leplyavkina, A. Livke, S. J. Luke, D. MacArthur, S. Razinkov, D. Sivachev, J. Thron, S. et al., "AVNG System Demonstration," 51st INMM Annual Meeting, Baltimore, MD, USA, 11–15 July 2010. It also holds for recent publications, see J. M. Mueller and J. Mattingly, "Passive One-dimensional Self-transmission Imaging of Subcritical Metallic Plutonium Assemblies,"

Nuclear Instruments and Methods in Physics Research A 903 (2018): 277–86; Pete Chapman, Jonathan Mueller, Jason Newby, and John Mattingly, "Exploiting Fission Chain Reaction Dynamics to Image Fissile Materials," *Nuclear Instruments and Methods in Physics Research A* 935 (2019): 198–206; and Eric Lepowsky, Jihje Jeon, and Alexander Glaser, "Confirming the Absence of Nuclear Warheads via Passive Gamma-Ray Measurements," *Nuclear Instruments and Methods in Physics Research A* 990 (2021): 164983.

10. The effect of HDPE on neutron multiplicity measurements was studied by E. C. Miller, B. Dennis, S.D. Clarke, S. A. Pozzi, and J. K. Mattingly, "Simulation of Polyethylene-Moderated Plutonium Neutron Multiplicity Measurements," *Nuclear Instruments and Methods in Physics Research A* 652 (2011): 540–43; its impact on detector efficiency by Mateusz Monterial, Peter Marleau, Marc Paff, Shaun Clarke, and Sara Pozzi, "Multiplication and Presence of Shielding Material from Time-Correlated Pulse-Height Measurements of Subcritical Plutonium Assemblies," *Nuclear Instruments and Methods in Physics Research A* 851 (2017): 50–6; and the effect of HDPE on fission chain distributions by G. Heger, C. Dubi, A. Ocherashvili, B. Petersen, and E. Gilad, "Identifying Neutron Shielding in Neutron Multiplicity Counting," *Nuclear Instruments and Methods in Physics Research A* 901 (2018): 40–5. Gamma signals produced by neutron activation in HDPE, which was placed in front of a detector, were addressed by Malte Göttsche, Janet Schirm, and Alexander Glaser, "Low-Resolution Gamma Ray Spectrometry for an Information Barrier Based on a Multi-Criteria Template-Matching Approach," *Nuclear Instruments and Methods in Physics Research A* 840 (2016): 139–44.
11. K. Böhnel, "The Effect of Multiplication on the Quantitative Determination of Spontaneously Fissioning Isotopes by Neutron Correlation Analysis," *Nuclear Science and Engineering* 90 (1985): 75–82; N. Ensslin, W. C. Harker, M. S. Krick, D. G. Langner, M. M. Pickrell, and J. E. Stewart, "Application Guide to Neutron Multiplicity Counting," LA-13422-M, 50–51, Los Alamos, NM, 1998.
12. Marc Looman, Paolo Peerani, and Hamid Tagziria, "Monte Carlo Simulations of Neutron Counters in Safeguards Applications," *Nuclear Instruments and Methods in Physics Research* A598 (2009): 542–50; P. Peerani, M. Swinhoe, A.L. Weber, and L. G. Evans, "ESARDA Multiplicity Benchmark Exercise," *ESARDA Bulletin* 42 (2009): 2–25.
13. Since attribute measurements monitor whether defined threshold values are met by the analyzed item, a limited bias could be taken into account by adjusting the thresholds accordingly.
14. Steve Fetter, Valery A. Frolov, Marvin Miller, Robert Mozley, Oleg F. Prilutsky, Stanislav N. Rodionov, and Roald Z. Sagdeev, "Detecting Nuclear Warheads," *Science & Global Security* 1 (1990): 225–302; G. Kessler, "Plutonium Denaturing by ^{238}Pu," *Nuclear Science and Engineering* 155 (2007): 53–73; Yoshiki Kamura, Masaki Saito, and Hiroshi Sagara, "Evaluation of Proliferation Resistance of Plutonium Based on Decay Heat," *Journal of Nuclear Science and Technology* 48 (2011): 715–23.
15. In "Detecting Nuclear Warheads," 232–50, passive and neutron-induced gamma and neutron flux densities were estimated; Huang Meng, Zhu Jianyu, Wu Jun, and Li Rui, "A Passive Method for the Detection of Explosives and Weapon-Grade Plutonium in Nuclear Warheads," *Science & Global Security* 26 (2018): 57–69 explored the potential of verifying the presence of high explosives by (n,γ) activation processes; Pierre-Luc Drouin, "Geant4 Simulation Study of Nuclear Weapon Detection Using a CLYC Detector," Defence Research and Development Canada, DRDC-RDDC-2018-R012

(2018) calculated photon spectra; and Moritz Kütt, Jan Elfes, and Christopher Fichtlscherer, "Fetter Model Revisited: Detecting Nuclear Weapons 30 Years Later," INMM & ESARDA Joint Virtual Annual Meeting, 23–26 August, 30 August–1 September 2021, simulated neutron fluxes within the configuration.

16. Another potential deliberate deception method could be to replace the core by other fissile material. Since such a hoax may not include explosives due to difficulties of adopting these to a differing geometry, as discussed in "A Passive Method for the Detection of Explosives and Weapon-Grade Plutonium in Nuclear Warheads," 58, this option has not been considered.
17. Partial exceptions are analyses of the AT-400R container on gamma and neutron correlation count rates from bare plutonium metal, Sara A. Pozzi, and John T. Mihalczo, "Monte Carlo Evaluation of Passive Correlation Measurements on Containerized Plutonium Shells," 44th INMM Annual Meeting, 13 July 2003, Phoenix, AZ, USA, and "Fetter Model Revisited" presenting neutron fluxes over component interfaces of the Fetter et al. model and of the energy spectrum of emitted neutrons.
18. When discussing the use of passive radiation measurements within IPNDV, representatives of a nuclear weapon state explained that according to their domestic safety regulations keeping 1 m distance from a fully assembled warhead is mandatory.
19. Irmgard Niemeyer, Jan Geisel-Brinck, Simon Hebel, Philip Kegler, Gerald Kirchner, Manuel Kreutle, and Stefan Neumeier, "Moving From Paper To Practice In Nuclear Disarmament Verification: NuDiVe–The Nuclear Disarmament Verification Exercise," 61. Annual Meeting Proceedings, Institute of Nuclear Materials Management, 12–16 July 2020, virtual.
20. "Detecting Nuclear Warheads," Appendix A, 255–63.
21. Nicholas J. Whitworth, "Modelling Detonation in Ultrafine TATB Hemispherical Boosters Using CREST," 17th Biennial International Conference of the APS Topical Group on Shock Compression of Condensed Matter, 26 June - 1 July 2011, Chicago, IL, USA, American Institute of Physics Conference Proceedings 1426 (2012): 213–16.
22. Pavel Podvig and Ryan Snyder, "Watch Them Go: Simplifying the Elimination of Fissile Materials and Nuclear Weapons," United Nations Institute for Disarmament Research (UNIDIR), Geneva, 2019, 28, https://doi.org/10.37559/WMD/19/NuclearVer01.
23. International Panel on Fissile Materials, "Global Fissile Material Report 2015: Nuclear Weapon and Fissile Material Stockpiles and Production," 2015, Appendix 1, 41–3, https://fissilematerials.org/publications/2015/12/global_fissile_material_report_7.html; Information on US W87 and W88 warheads in "The Nuclear Weapon Archive," https://nuclearweaponarchive.org/ have been used also.
24. "Detecting Nuclear Warheads," 238.
25. Except for the slightly larger dimensions it corresponds to the ALR8 container, which in the United States has been used for storage of ex-weapon plutonium pits, see Yevgeni V. Terekhine, Theodore A. Parish, and William S. Charlton, "Shielding and Criticality Characterization of ALR8(SI) Plutonium Storage Containers," *Journal of Nuclear Science and Technology* 37, sup 1 (2000): 347–51; we disregarded the steel insert present in the ALR8(SI) version for corrosion prevention.
26. S. Agostinelli, J. Allison, K. Amako et al., "GEANT4–A Simulation Toolkit," *Nuclear Instruments and Methods in Physics Research* A 506 (2003): 250–303; J. Allison, K. Amako, J. Apostolakis, P. Arce, M. Asai, T. Aso, E. Bagli, A. Bagulya, S. Banerjee, G. Barrand, et al., "Recent Developments in GEANT4," *Nuclear Instruments and Methods in Physics Research* A 835 (2016): 186–225.

27. Examples illustrating the range of topics addressed with Geant4 are: A. Sh. Georgadze, "Monte Carlo Simulation of Active Neutron Interrogation System Developed for Detection of Illicit Materials," *Acta Physica Polonica B* 48 (2017): 1683–91; Lin Zhuang, Quanhu Zhang, Wenming Zuo, and Chen Chen, "Computer Simulation of Fast Neutron Multiplicity Analysis," *Advances in Engineering Research* 129 (2017): 225–30; "Geant4 Simulation Study of Nuclear Weapon Detection Using a CLYC Detector"; Daniel C. Poulson, "Interrogation of Spent Nuclear Fuel Casks Using Cosmic-Ray Muon Computed Tomography," PhD Dissertation (2019), University of New Mexico, https://digitalrepository.unm.edu/ne_etds/90.
28. Jérôme M. Verbeke, Chris Hagmann, and Doug Wright, "Simulation of Neutron and Gamma Ray Emission from Fission and Photofission," UCRL-TR-228518-REV-1, Livermore, California, 2016, https://nuclear.llnl.gov/simulation/fission.pdf.
29. Peter J. Karpius, William Clay, Katherine C. Frame, Duncan MacArthur, Peter Santi, Morag K. Smith, and Jonathan Thron, "Monte Carlo Simulations and Data Comparison for Liquid-Scintillator Detectors to be Used in a Multiplicity Counter," 48th Annual INMM Meeting, 8–12 July 2007, Tuczon, AZ, USA; B. M. van der Ende, J. Atanackovic, A. Erlandson, and G. Bentoumi, "Use of Geant4 vs. MCNPX for the Characterization of a Boron-Lined Neutron Detector," *Nuclear Instruments and Methods in Physics Research A* 820 (2016): 40–7; Jiawei Tan and Joseph Bendahan, "Geant4 Modifications for Accurate Fission Simulations," *Physics Procedia* 90 (2017): 256–65; H. N. Tran, A. Marchix, A. Letourneau, J. Darpentigny, A. Menelle, F. Ott, J. Schwindling, and N. Chauvin, "Comparison of the Thermal Neutron Scattering Treatment in MCNP6 and GEANT4 Codes," *Nuclear Instruments and Methods in Physics Research A* 893 (2018): 84–94; R. Sarwar, V. Astromskas, C. H. Zimmerman, G. Nutter, A. T. Simone, S. Croft, and M. J. Joyce, "An Event-Triggered Coincidence Algorithm for Fast-Neutron Multiplicity Assay Corrected for Cross-Talk and Photon Breakthrough," *Nuclear Instruments and Methods in Physics Research A* 903 (2018): 152–61.
30. These include the resolved and unresolved resonance regions as well as thermal scattering, see L. Thulliez, C. Jouanne, and E. Dumonteil, "Improvement of Geant4 Neutron-HP package: From Methodology to Evaluated Nuclear Data Library," *Nuclear Instruments and Methods in Physics Research A* 1027 (2022): 166187 and references therein.
31. International Criticality Safety Benchmark Evaluation Project, "International Handbook of Evaluated Criticality Safety Benchmark Experiments," NEA 7520, OECD Nuclear Energy Agency, Paris, 2020.
32. For this purpose we modified Geant4 to track and store the numbers of fission neutrons produced per simulated generation.
33. Christopher. J. Werner, editor, "MCNP User's Manual, Code Version 6.2," LA-UR-17-29981, Los Alamos, NM, USA, 2017.
34. B. T. Rearden and M. A. Jessee, editors, "SCALE Code System," ORNL/TM-2005/39, version 6.2.3, Oak Ridge, TN, USA, 2018.
35. Manuel Kreutle, Alessandro Borella, Riccardo Rossa, Celine Scholten, Gerald Kirchner, and Claas van der Meer, "Benchmarking Monte Carlo Simulations in the Context of Nuclear Disarmament Verification via Monte Carlo Simulations with GEANT4," INMM & ESARDA Joint Virtual Annual Meeting, 23–26 August & 30 August-1 September 2021.
36. United Nations Scientific Committee on the Effects of Atomic Radiation, "UNSCEAR 2000 Report to the General Assembly," Volume I, Annex B, 86 gives a value of $0.013\,\mathrm{cm}^{-2}\ \mathrm{s}^{-1}$ at sea level, which will be smaller in buildings, but may show an

increased level in a nuclear weapons maintenance facility, https://www.unscear.org/unscear/en/publications/2000_1.html.

37. See note 8 above.
38. See note 11 above.
39. A similar effect is caused within bare plutonium by hydrogeneous material present in a storage container, Malte Göttsche, Paolo Peerani, and Gerald Kirchner, "Concepts for Dismantlement Verification and Neutron Multiplicity Measurements for Plutonium Mass Attribute Determination," 35th ESARDA Annual Meeting, 27–30 May 2013, Bruges, Belgium, May Proceedings, EUR-26127 (2013): 477–85.
40. See note 8 above.
41. Nicholas Reed, Anders Axelsson, Gerald Kirchner, Sakari Ihantola, Manuel Kreutle, Kari Peräjärvi, and Antonin Vacheret, "nFacet 3D: Fission Neutron Measurements With A Segmented Scintillation Detector," Proceedings of the INMM & ESARDA Joint Virtual Annual Meeting, 23–26 August, 30 August–1 September 2021.
42. A concept for realizing this is developed by Svenja Sonder, Simon Hebel, Carina Prünte, and Gerald Kirchner, "Impact of Concrete Building Structures on Neutron Radiation," *ESARDA Bulletin* 64 (2022): 2–9.
43. These include calorimetry and for warheads without tamper gamma spectrometry.
44. This value follows from the neutron die-away times within the helium-3 detectors of about 50 µs, "Application Guide to Neutron Multiplicity Counting," 17.
45. With $8.89 \cdot 10^4$ spontaneous fissions per second and a typical detector efficiency of 40 percent signals of the bare plutonium are separated by about 30 µs on average.
46. "Transparency and Verification Options," 62–71.
47. "Confirming the Absence of Nuclear Warheads via Passive Gamma-Ray Measurements," 2–3.
48. "Monitoring Nuclear Weapons and Nuclear-Explosive Materials," 101–2.
49. The exception would be the case of a single tamper including type, since its template will significantly differ from the others.
50. T. Douglas Reilly, "Passive Nondestructive Assay of Nuclear Materials. 2007 Addendum," 11–14, Los Alamos, New Mexico, 2007, https://www.lanl.gov/org/ddste/aldgs/sst-training/_assets/docs/PANDA %202007%20Addendum/0.%20PANDA%20Preface%20v1-3.pdf.
51. With an effective detection area of 25 cm^2 and an absolute efficiency of 10% as typical for HPGe detectors at the energies of interest, the accumulation of 100 counts for the 642 keV plutonium-240 line will take roughly 2.4 hours; taking into account the background of 142 counts caused by Compton scattering of uranium decay gammas with energies above 642 keV, the measurement will result in a statistical uncertainty of 18.5%.
52. For the United States, a mean radium-226 concentration in soil of 40 Bq kg^{-1} is given with a range of 8–160 Bq kg^{-1}, "UNSCEAR 2000 Report to the General Assembly," Volume I, Annex B, 115.
53. Steve Fetter, Thomas B. Cochran, Lee Grodzins, Harvey L. Lynch, and Martin S. Zucker, "Gamma-Ray Measurements of a Soviet Cruise-Missile Warhead," *Science* 248 (1990): 828–34.
54. "Confidence, Security and Verification," 19; "Monitoring Nuclear Weapons and Nuclear-Explosive Materials," 105; (n,γ) lines present in the gamma spectra recorded during the Black Sea experiment could originate from activation of high explosives, but also of cruise missile fuel, "Gamma-Ray Measurements of a Soviet Cruise-Missile Warhead," 829.
55. "A Passive Method for the Detection of Explosives and Weapon-Grade Plutonium in Nuclear Warheads," 64.

56. See note 36 above.
57. This will allow to verify the absence of the shielded plutonium with commercially available multiplicity counters such as the High-Efficiency Neutron Counter, see H. O. Menlove, J. Baca, J. M. Pecos, D. R. Davidson, R. D. McElroy, and D. B. Brochu, "HENC Performance Evaluation and Plutonium Calibration," LA-13362-MS, Los Alamos, NM, USA, 1997.

Appendix A

Table A1. Specification of the primaries of the two notional weapon models used; if not otherwise noted, data of configuration 1 were adopted from Fetter et al.[a]

	Configuration no.	
	1	2
Fissile material	Plutonium	
- Mass [kg]	4.0	
- Composition [weight-percent]		
Plutonium-239	95.0	
Plutonium-240	4.7	
Plutonium-241	0.1	
Americium-241	0.2	
- Geometry	Hollow sphere	
- Inner radius [cm]	4.25	
- Outer radius [cm]	5.0	
Reflector	Beryllium	
- Thickness [cm]	2.0	
Tamper	Natural uranium	—
- Thickness [cm]	3.0	—
High explosive	TATB	
- Density[b] [g cm^{-3}]	1.80	
- Thickness [cm]	10.0	12.44
Casing	Aluminum	
- Thickness [cm]	1.0	

[a]"Detecting Nuclear Warheads," Appendix A, 255–263. [b]"Modelling Detonation in Ultrafine TATB Hemispherical Boosters Using CREST," 213.

Table A2. Assumptions made for the notional thermonuclear weapon model (Configuration 2).

Spark plug	High enriched uranium
- Mass [kg]	3.0
- Geometry	Sphere
- Radius [cm]	3.35
Pusher	High enriched uranium
- Mass [kg]	17.0
- Geometry	Hollow sphere
- Inner radius [cm]	14.68
- Outer radius [cm]	15.0
Fusion material	Lithium deuteride
- Lithium-6 enrichment [%]	95.0
- Density[a] [g cm^{-3}]	0.83
Distance from primary	
- Center to center [cm]	45.0
Plastic foam	Polystyrene
- Density[b] [g cm^{-3}]	0.022
Inner casing	Natural uranium
- Radius [cm]	19.9
- Thickness [cm]	0.1
Air gap	
- Thickness [cm]	0.5
Outer casing	Aluminum
- Thickness [cm]	1.0

[a]This was calculated from the density of lithium hydride of 0.82 g cm^{-3} specified in the Pacific Northwest National Laboratory Compendium of Material Composition Data for Radiation Transport Modeling, PNNL-15870, Rev. 2, 2021, 146 by taking into account the differing isotopic weights. [b]This follows from 98 volume-percent of air being present in the polystyrene with density of 1050 kg m^{-3}, https://material-properties.org/polystyrene-density-strength-melting-point-thermal-conductivity/.

Table A3. Materials and geometries assumed for the shielded plutonium in the scrap container scenario.

(a) Scrap	
Composition [vol.-percent]	
- Iron	10
- Plastics	5
- Aluminum	5
- Air	80
Density[a] [g cm^{-3}]	0.986
(b) Container	
Material	Stainless steel
Inner diameter [mm]	583.6
Outer diameter [mm]	585
Height [mm]	880

This value is close to the mean density derived from an extensive survey of the metal scrap market in Germany, see Oleg Sobolev, Stefan Wörlen, Joost de Groot, J. Iloff, Kirsten Haneke, and Talianna Schmidt, "Experimental and theoretical studies on radioactive sources and objects in metal scrap–Project 3615S52320," (in German), Federal Office for Radiation Protection (2019), http://nbn-resolving.de/urn:nbn:de:0221-2019052818209.